Journal Pre-proof

Removal of lead ions from wastewater using lanthanum sulfide nanoparticle decorated over magnetic graphene oxide

Shahabaldin Rezania, Amin Mojiri, Junboum Park, Nicole Nawrot, Ewa Wojciechowska, Najat Marraiki, Nouf S.S. Zaghloul

PII: S0013-9351(21)01254-8

DOI: https://doi.org/10.1016/j.envres.2021.111959

Reference: YENRS 111959

To appear in: *Environmental Research*

Received Date: 30 June 2021

Revised Date: 18 August 2021

Accepted Date: 22 August 2021

Please cite this article as: Rezania, S., Mojiri, A., Park, J., Nawrot, N., Wojciechowska, E., Marraiki, N., Zaghloul, N.S.S., Removal of lead ions from wastewater using lanthanum sulfide nanoparticle decorated over magnetic graphene oxide, *Environmental Research* (2021), doi: https://doi.org/10.1016/j.envres.2021.111959.

Title: Removal of lead ions from wastewater using lanthanum sulfide nanoparticle decorated over magnetic graphene oxide

Shahabaldin Rezania*: Writing - original draft, Methodology

Amin Mojiri: Writing - review & editing, Software

Junboum Park: Resources; Visualization

Nicole Nawrot: Writing - review & editing,

Ewa Wojciechowska: Conceptualization;

Najat Marraiki: Writing - review & editing

Nouf S. S. Zaghloul: Validation, Formal analysis

Removal of lead ions from wastewater using lanthanum sulfide nanoparticle decorated over magnetic graphene oxide

Shahabaldin Rezania[1]*, Amin Mojiri[2], Junboum Park[3], Nicole Nawrot[4] , Ewa Wojciechowska[4], Najat Marraiki[5], Nouf S. S. Zaghloul[6]

[1]*Department of Environment and Energy, Sejong University, Seoul 05006, South Korea*

[2] *Department of Civil and Environmental Engineering, Graduate School of Advanced Science and Engineering, Hiroshima University, 1-4-1 Kagamiyama, Higashihiroshima 739-8527, Japan*

3 Department of Civil and Environmental Engineering, Seoul National University, Seoul, South Korea

4 Gdańsk University of Technology, Faculty of Civil and Environmental Engineering, Narutowicza 11/12, 80-233 Gdańsk, Polnad

[5]*Department of Botany and Microbiology, College of Science, King Saud University, P.O. 2455, Riyadh, 11451, Saudi Arabia.*

[6]*Bristol Centre for Functional Nanomaterials, HH Wills Physics Laboratory, Tyndall Avenue, University of Bristol, Bristol, BS8 1FD, UK*

*Corresponding author Email: (shahab.rezania@sejong.ac.kr)

Acknowledgment

The authors extend their appreciation to the Researchers Supporting Project number (RSP-2021/201), King Saud University, Riyadh, Saudi Arabia.

This study is not dealing on human subjects or experimental animals,

Abstract

In this study, the new lanthanum sulfide nanoparticle (La_2S_3) was synthesized and incorporated onto magnetic graphene oxide (MGO) sheets surface to produce potential adsorbent (MGO@LaS) for efficient removal of lead ions (Pb^{2+}) from wastewater. The synthesized MGO@LaS adsorbent was characterized using Fourier transform infrared spectroscopy, field emission scanning electron microscopy and energy-dispersive X-ray spectroscopy. The effective parameters on the adsorption process including solution pH (~5), adsorbent dosage (20 mg), contact time (40 min), initial Pb^{2+} concentration and temperature were studied. The removal effeciency was obtained > 95 % for lead ions at pH 5 with 20 mg adsorbent. To validate the adsorption rate and mechanism, the kinetic and thermodynamic models were studied based on experimental data. The Langmuir isotherm model was best fitted to initial equilibrium concentration with a maximum adsorption capacity of 123.46 mg/g. This indicated a monolayer adsorption pattern for Pb^{2+} ions over MGO@LaS. The pseudo-second-order as the kinetic model was best fitted to describe the adsorption rate due to high $R^2 > 0.999$ as compared first-order. A thermodynamic model suggested a chemisorption and physisorption adsorption mechanism for Pb^{2+} ions uptake into MGO@LaS at different temperatures; $\Delta G° < –5.99$ kJ $mol^{–1}$ at 20 °C and $\Delta G°$ -18.2 kJ $mol^{–1}$ at 45 °C. The obtained results showed that the novel nanocomposite (MGO@LaS) can be used as an alternative adsorbent in wastewater treatment.

Keywords: lanthanum sulfide nanoparticles, magnetic graphene oxide, lead ions removal, adsorption equilibrium, and adsorption kinetic.

1. Introduction

In the past few decades, heavy metals have become one of the biggest challenges to the aquatic environment (Gabris et al., 2018; Madhavan et al., 2019; Tan et al., 2020). Long exposure to heavy metal ions can cause neurodegenerative disorders, liver and kidney failure, and cancer in mammals (Fu and Xi, 2020; Paithankar et al., 2021). Lead (Pb^{2+}) ions are one of the main heavy metal ions that are most harmful, toxic, and carcinogenic as well as are responsible for various

antagonistic effects on tissues, and living beings (Anyakora, 2010; Rashidi Nodeh et al., 2020b; Yu et al., 2021). In this regard, the EPA guideline adjusted the maximum residual limit level for lead ions less than 50 µg/L in wastewater and 10 µg/L in drinking water (Arbabi et al., 2015). Hence, the remediation of lead ions from the environmental water before discharge into the environment is an important task.

In the past few decades, different techniques have been applied for organic toxic species and inorganic heavy metal ions removal from aqueous media including bioremediation, photocatalytic, membrane, polymers, electro-coagulation, oxidative degradation and adsorption (Chai et al., 2021; Kamboh et al., 2021; Leong and Chang, 2020; Senthil et al., 2018). Among these, adsorption is a remarkable technique for the removal of lead ions from water samples, which is environmentally friendly, simple operation, ease of recovery, low cost, quickly effective, easy, environmentally friendly and does not produce secondary pollutants in water (Wan Ibrahim et al., 2016). In the adsorption technique, the adsorbent is a core factor that directly affects the adsorption capacity, selectivity, and removal efficiency (Wu et al., 2020). Hence, researchers employed various adsorbents for heavy metal ions removal including, carbon-based material, agriculture biomass, zeolite, silica, metal-organic-framework, polymeric beads, biopolymers (Chakraborty et al., 2020; Duan et al., 2020). Recently newly developed carbon-based material (activated carbon, MWCNTs and graphene) is widely used for the removal of heavy metal ions and lead ions due to its high chemical stability, high surface area, and various oxygenated functional groups (Naik et al., 2021; Rajivgandhi et al., 2021; Zhang et al., 2020). In addition, graphene is a two-dimensional material that both sides of flake sheets are available for the adsorption process (Muthusaravanan et al., 2021). However, further modification of graphene oxide is needed to increase the adsorptive affinity toward lead ions with high adsorption capacity (Jun et al., 2019; Lai et al., 2020).

According to the literature, metallic cation-anion nanoparticles are considered as the potential adsorbent material for the adsorption of lead ions from water via electrostatic and electron sharing mechanisms (Golkhah et al., 2017; Zhao et al., 2019). In particular, the sulfide anions (S^{2-}) rich bimetallic materials are superior and flexible materials in adsorption/removal approaches (Prabhu et al., 2019; Theerthagiri et al., 2017). Since, the presence of sulfide over adsorbent material can create hydrogen bonding with target pollutants as well as increase the hydrophilicity of the adsorbent (Patil and Lokhande, 2015; Rashidi Nodeh et al., 2020a). Various

types of sulfide-metal cations such as iron sulfide and nickel sulfide are relatively inexpensive material which has high efficiency for the removal of lead ion (Ahmadi et al., 2015; Golkhah et al., 2017; Zhao et al., 2019). Besides, the trivalent lanthanum ions (La^{3+}) have a high potential for oxygen-donor atoms with sulfur ions which resulted in the formation of lanthanum sulfide (La_2S_3) nanoparticles (Rashidi Nodeh et al., 2020a). The La_2S_3 nanoparticles are superior and flexible material for the adsorption of various pollutants from the aquatic environment (Li et al., 2020; Prabhu et al., 2019; Rashidi Nodeh et al., 2020a).

The novelty of work is stated that the fewer studies were focused on the synthesizing, characterization and application of lanthanum sulfide (La_2S_3) NPs based magnetic graphene oxide material for lead adsorption. This material enhance the lead ions with high sorption capacity, since, The graphene oxide sheets with high surface area avoid the agglomeration and sedimentation of La_2S_3 nanoparticles. More active sices (LaS NPs) are available for lead ions uptake from aqueous media. Furthermore, the positively charged lanthanum ions (La^{3+}) and negative sulfide ions (S^{2-}) increase the adsorbent affinity toward lead ions. The most important strategy, the negatively charged sulfide-based nanoparticles are useful for the removal of the positively charged metal cations (Pb^{2+}). Besides, the presence of magnetic nanoparticles helps to easily isolation of nanocomposites from aqueous media (Ramu et al., 2020). Therefore, in this study, the La_2S_3 NPs were anchored over magnetic GO for the first time as new adsorbent material for the efficient removal of lead ions from wastewater.

2. Experimental

2.1 Reagents and chemicals

Potassium permanganate, $LaCl_3.7H_2O$, and $Na_2S_2O_3.5H_2O$, sodium hydroxide, ammonia solution 25%, sulfuric acid 98%, $FeCl_2.4H_2O$, $FeCl_3.6H_2O$, and other reagents were purchased from Merck Chemicals (Darmstadt, Germany). Synthetic graphene was obtained from Sigma Aldrich (Inc. St. Louis, MO, USA).

2.2 Instruments

The FT-IR spectra of the nanocomposite were recorded in the wavenumber range of 450 to 4000 cm^{-1} using a Perkin Elmer Spectrum 2 (Shelton, CT, USA). The surface morphology of the

nanocomposite material is investigated with a field emission scanning electron microscope from MIRA3 TESCAN (Prague, Czech Republic). The SEM instrument was equipped with energy-dispersive X-ray spectroscopy for analyzing the elemental composition of the nanocomposite. A Perkin Elmer 400 atomic absorption spectrophotometer (FAAS) equipped with lead hollow cathode lamps was used for the detection of lead ions in water samples.

2.3 Synthesis nanocomposite

Firstly, graphene oxide was synthesized from graphite according to previous studies the magnetized (Wu et al., 2019). Synthesis of magnetic graphene oxide (MGO) can be summarized as follows (Fig. 1); freshly prepared graphene oxide 1 g was mixed with 0.5 g of $FeCl_3.6H_2O$ and 0.25 g of $FeCl_2.4H_2O$ in 50 mL distilled water. Then, 3 mL of ammonia (25%) was added followed by vigorous stirring for 2 h. The dark product (MGO) was collected via a magnet, washed with excess distilled water and lastly oven-dried at 80ºC for 24 h. The Lanthanum sulfide (La_2S_3) nanoparticles over MGO were prepared by adaption of the method as previously reported by (Rashidi Nodeh et al., 2020a) as follows (Fig. 1); 0.35 g of $LaCl_3.7H_2O$, 0.78 g of $Na_2S_2O_3.5H_2O$ and 0.5 g MGO were mixed in 10 mL polyethylene glycol - 400 with vigorous stirring on heater stirrer at 80 °C for 30 min. The mixture was capped in a pyrex vial (20 mL) and heated in an oven at 120 °C for 24 h. Lastly, the dark black sediment (MGO@LaS) was isolated with the assistance of an external magnet and excess water with ethanol and distilled water five times and oven-dried at 80 °C for 24 h.

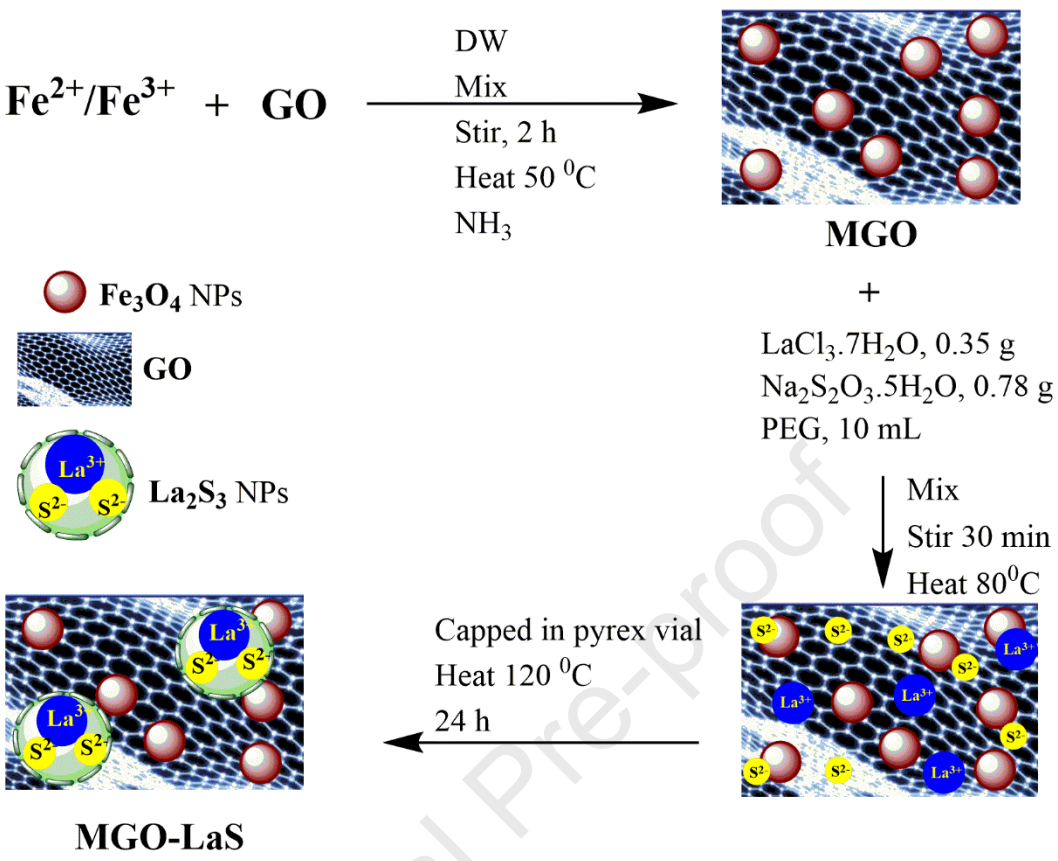

Fig. 1 Synthesis procedure for the magnetic graphene oxide doped lanthanum sulfide nanoparticles (MGO@LaS)

2.4 Removal experiment

The removal/adsorption of lead ions was carried out via batch method with different initial concentrations of lead ions (5 - 200 mg/L). The mass transfer of lead ions into MGO@LaS was enhanced by shaking for different times (10 -300 min). The pH of the solution was vireos from 2 to 7 by constant shaking rate and time. In a further study, the different effects of adsorbent dosage (5 -100 mg) and solution temperature (20 – 45 ºC) were investigated under constant shaking. All the experiments were carried out in triple and the concentration of residual lead ions in solution was analyzed with flame atomic absorption spectroscopy (FAAS). The removal efficiency (*R %*) of the lead ions was calculated according to equation (1).

$$R\ \% = \frac{C_i - C_e}{C_i} \times 100 \qquad (1)$$

Where C_i *(mg/L)* and C_e *(mg/L)* are the initial and residual concentrations of lead ions in solution, respectively. The equilibrium adsorption capacity (Q_e) was calculated under equation 2.

$$Q_e = \frac{(C_i - C_e) \times V}{W} \qquad (2)$$

Where C_i (mg/L) is the initial concentration of lead before treatment, V (mL) is the water phase volume and W is the adsorbent dosage (g). The effect of coexisting ions on lead ions removal was carried out using an artificial water solution including various anions and cations including SO^{3-}, NO_3^-, K^+, PO^{4-}, Fe^{3+}, Cl^-, Cu^{2+}, Na^{2+}, Zn^{2+} Ni^{2+}, and Al^{3+}. These concentration ions kept 10 folds of lead ions (200 mg/L) and mixed with 40 mL wastewater with a lead ions concentration of 21 mg/L. The removal was provided in single batch mode and the concentration of lead ions was analyzed with FAAS.

3. Results and discussion

3.1 Characterization

3.1.1 SEM and EDX

The FESEM microscopy was applied for the morphological study of the freshly prepared GO, La_2S_3 nanoparticles, and MGO@LaS nanocomposite. Fig. 2(A) shows the flake-like sheets for graphene oxide before modification and magnetization. Fig. 2(B) illustrates the SEM image of the La_2S_3 nanoparticles with irregular shape and size with agglomerated particles. It can be concluded that the graphene oxide sheets are prevented the agglomeration of the lanthanum sulfide nanoparticles as compared to graph (B). Fig. 2(C) depicts the SEM micrograph of the magnetic graphene oxide-based lanthanum sulfide nanocomposite after modification. In this graph, the uniform and smooth surface morphology was observed for nanoparticles over graphene oxide layers. In further characterization, the elemental composition of the MGO@LaS nanocomposite was analyzed with the EDX technique as shown in Fig. 2(D). The spectrum showed the various signal for the expected elements including C (31 %), O (21 %), Fe (19 %), S (13 %) and La (15 %). The proposed elements were matched with the material of MGO@LaS nanocomposite.

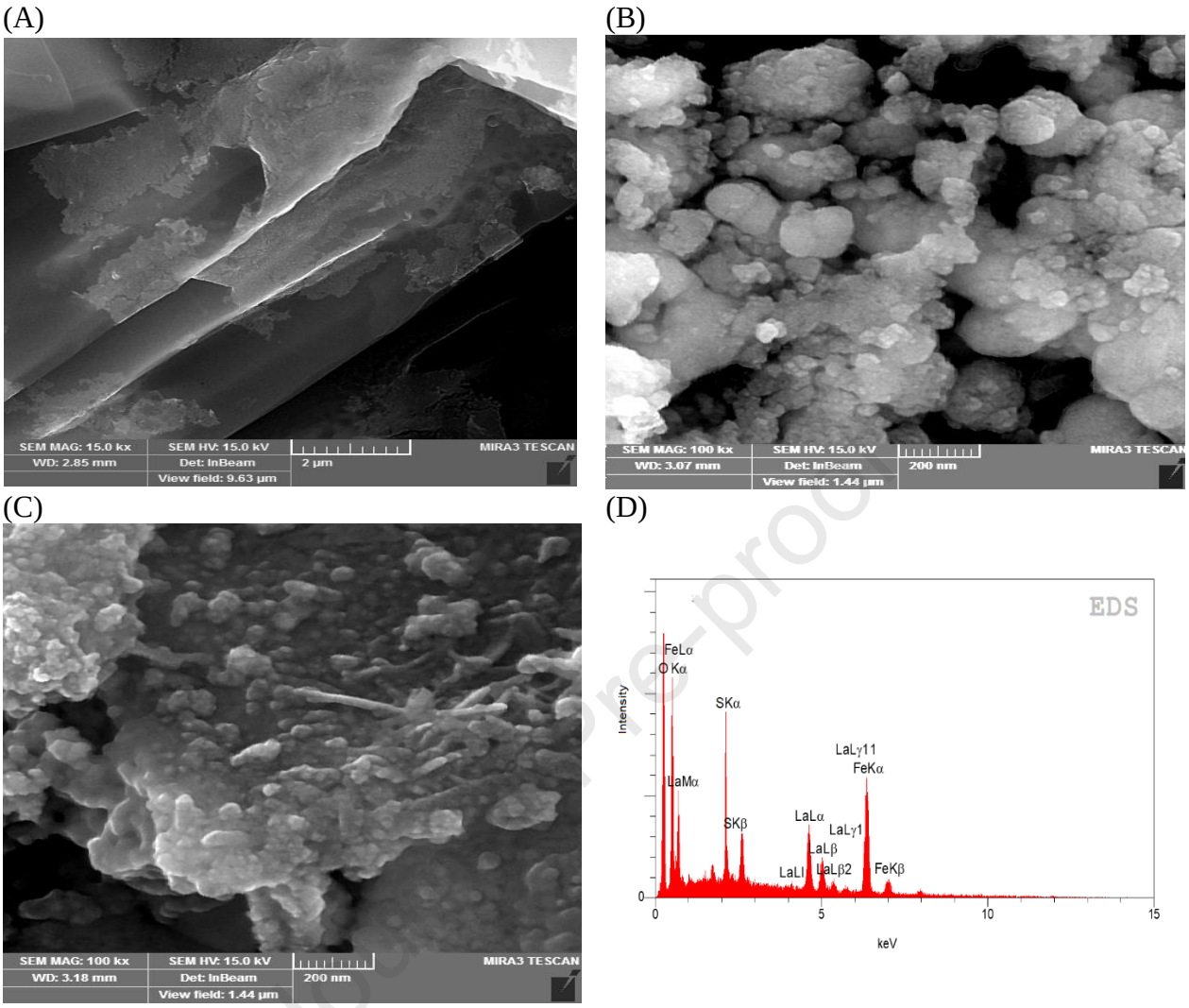

Fig. 2 SEM images for (A) graphene oxide, (B) lanthanum sulfide and (C) MGO@LaS nanocomposite. (D) EDX elemental analysis of MGO@LaS nanocomposite.

3.1.2 FTIR spectroscopy

The functional groups of MGO@LaS nanocomposite were studied with FTIR spectroscopy. Fig. 3(A) spectrum shows the main characteristic peaks for GO at 3410 cm^{-1}, 2925 cm^{-1}, 1722 cm^{-1}, 1630 $cm^{-}1$, 1495 cm^{-1}, 1208 cm^{-1}, and 1029 cm^{-1} which were corresponded to carbonyl O-H, C-H, C=O, C=C, C-C, C-O, and C-OH stretching vibrations, respectively. These showed the presence of various oxygenate functional groups on the surface of graphene oxide. Hence, the extra IR bands at 625 cm^{-1}, 945 cm^{-1}, and 2314 cm^{-1} corresponded to La–S, La_2S_3 nanoparticles, and S–H & S–S residual, respectively (Rashidi Nodeh et al., 2020a). The IR bands are proximately at 930 cm^{-1} and 750 cm^{-1} corresponds to sulfide and sulfur-based materials such as

metal-sulfide and SO_3^{2-} (Brandão et al., 2009; Pandian et al., 2011; Rashidi Nodeh et al., 2020a). lastly, the sharp bond at 562 cm^1 was attributed to the Fe-O bond vibration stretching of magnetic nanoparticles. Hence, these peaks verified the successful assembly of graphene oxide sheets with magnetic nanoparticles and La_2S_3 nanoparticles.

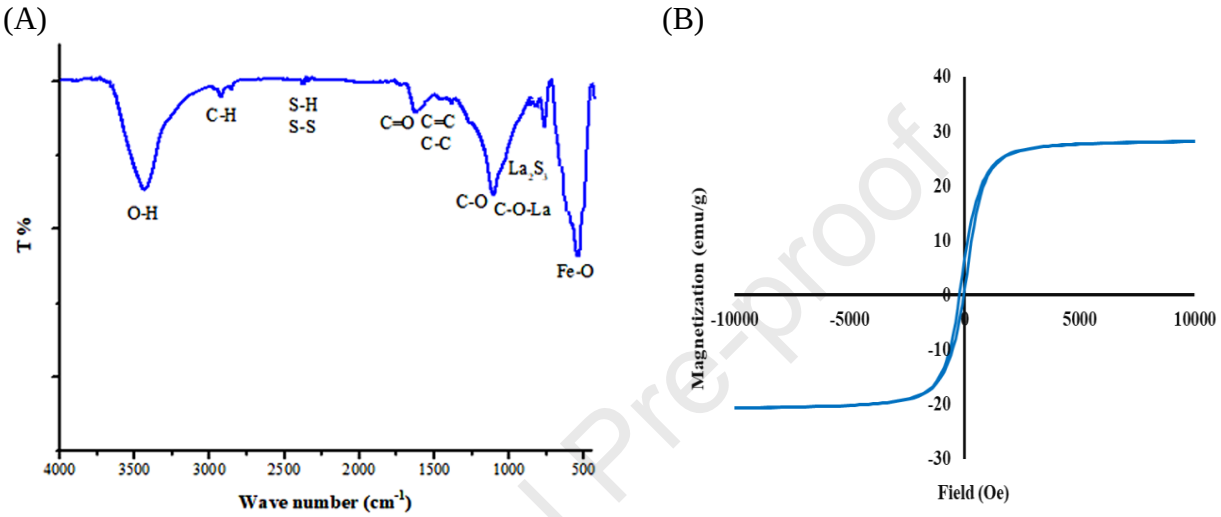

Fig. 3 (A) FTIR spectrum for MGO@LaS nanocomposite. (B) VSM hystrisis for MGO@LaS nanocomposite.

3.1.3 VSM magnetometery

the magnetic properties of adsorbent were studied vibrating sample magnetometer (VSM) technique. The VSM showed the magnetic saturation capacity for adsorbent material which is an important parameter in the magnetic adsorption removal techniques (Shirani et al., 2021). Fig. 3 (B) showd the VSM curve for MGO@LaS nanocomposite with asymmetric hysteresis and the saturation magnetization of 26 emu/g. This value was illustrated that MGO@LaS had a worthy magnetic properties which made it suitable for the treatment of wastewater.

3.2 Adsorption mechanism

The proposed mechanism for Pb^{2+} ions uptake onto MGO@LaS nanocomposites is shown in Fig. 4. The Pb^{2+} ions can adsorb over sulfur, nitrogen and oxygen atoms via electrostatic interactions and coordination mechanisms. As can be seen, the Pb^{2+} ions interacted with the electron pair of *S* atom in lanthanum sulfide and *O* atom in MGO as donor atoms to form complex or physical adsorption via electrostatic interaction. Hence, due to the high value of *S* atom and the high affinity of the lead ions to interact with sulfur, coordination was highly possible between the Pb^{2+} ions and lanthanum sulfide. Electrostatic interactions were more possible between oxygenate groups of MGO and Pb^{2+} ions. Therefore, the presence of various force interactives in the adsorption process provides the synergic effect to increase the removal efficiency.

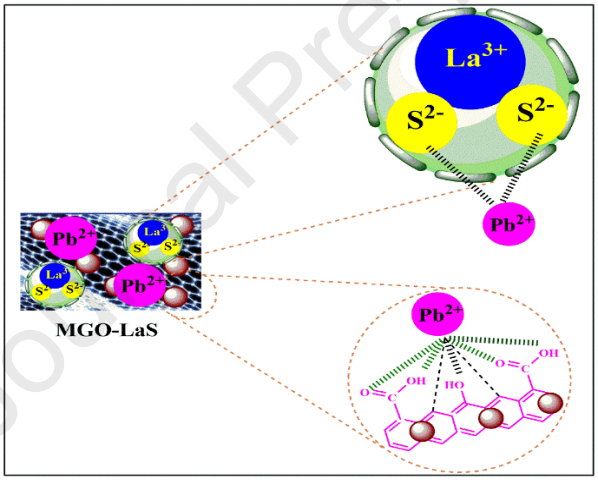

Fig. 4 The proposed mechanism for adsorption of Pb(II) ions onto MGO@LaS nanocomposite.

3.3 Effect of parameters on adsorption process

3.3.1 Solution pH

The effect of different pH on the removal of Pb^{2+} was evaluated at pHs 2-7. As shown in Fig. 5(A), the removal efficiency increased from pH 2 to 5, probably due to the presence of a large value of negative S^{2-} on the surface of the MGO@LaS nanocomposite. Since positively charged Pb^{2+} can be readily adsorbed via electrostatic attraction at pH 2-5 over nanocomposite. However,

the low efficiency at low pH was probably due to the protonation of the adsorbent that occupies the active sites. This phenomenon increases the electrostatic repulsion between the Pb^{2+} cations and protonated adsorbents (MGO^{+} & LaS-H). The maximum removal efficiency was achieved at pH 5, which was due to the high affinity between the negative surface charge of the nanocomposite and positive Pb^{2+} cations. The small decline in efficiency at pH 6 and 7 was because of the precipitation of lead ions as hydroxide ($Pb(OH)_2$) then, pH> 7 was not studied. Hence, the pH of the adsorption batch was set at 5 for further studies, as the number of negatively charged sites was high on the surface of $MGO@LaS^{-}$, which is suitable for the efficient uptake of the positive Pb^{2+} ions by electrostatic attraction or coordination.

3.3.2 Adsorbent dosage

The effect of adsorbent dosage on lead ions removal was studied in the mass range of 5-100 mg. Fig 5(B) shows the removal efficiency of lead ions increased from 39% to 95% by increasing the adsorbent dosage from 5 to 30 mg. This increase was due to the increasing adsorption active sites on the adsorbent. As can be seen, the adsorption capacity (Q_e) was continuously decreased by increasing the mass of the adsorbent. The decline of Q_e is probably due to the decreasing amount of metal ions concentration per unit mass of adsorbents (adsorbate/active sites ratio is decreasing), which causes unsaturation of some adsorption active sites (Kakavandi et al., 2015). Thus, 20 mg was chosen as an effective dosage for further study.

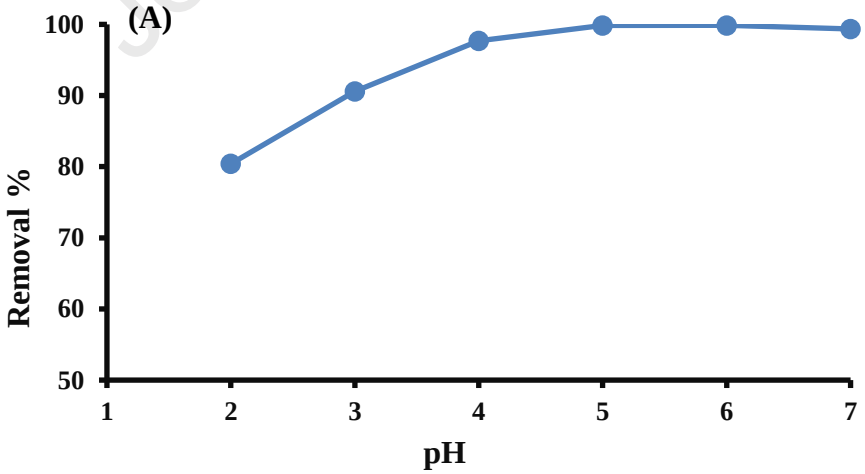

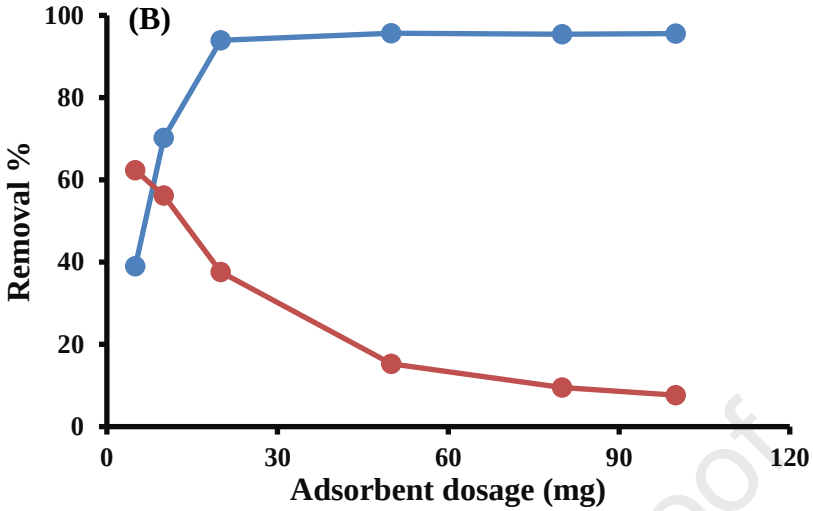

Fig. 5 Effect of (A) solution pH and (B) adsorbent dosage on adsorption efficiency.

3.3.3 Effect of the contact time

Batch experiments were conducted on a shaker for different interval contact times (5-300 min) to get equilibrium sorption capacity using 40 mL lead ions solution and 50 mg of adsorbent at pH 5. Fig. 6 shows the removal efficiency increased continuously by increasing the shaking time. This trend was assigned to the longer time available for more removal to occur with greater contact times. Hence, the efficient and fast removal of Pb^{2+} ions is corresponding to a large number of the active sites (various functional groups) that cause a fast equilibrium and mass transfer between solution and adsorbent (Li et al., 2015). Thus, 40 min was selected for further experimental works.

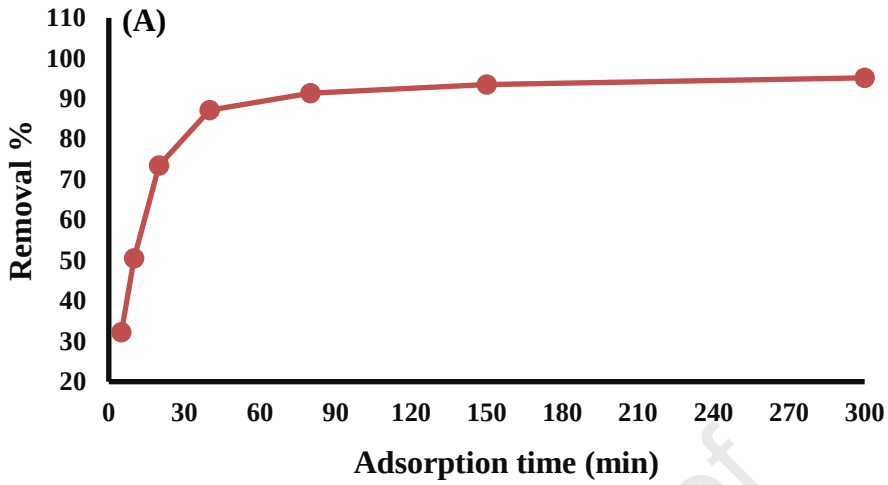

Fig. 6 Effect of adsorption time on removal efficiency

3.3 Adsorption kinetic

The experimental process and mass transfer rate for the adsorption process were analyzed using the pseudo-first-order and pseudo-second-order as kinetic models (Mousavi et al., 2019). The proposed two models are described with linear equations (3) and (4) respectively (Esmaeili Bidhendi et al., 2020), which are plotted in Fig. 6 A & B.

$$\ln(Q_e - Q_t) = \ln Q_e - k_1 t \qquad (3)$$

$$t/Q_t = 1/(k_2 Q_e^{\,2}) + t/Q_e \qquad (4)$$

Where Q_e (mg/g) equilibrium adsorption capacity (mg/g) and Q_t (mg/g) are the capacities at a certain time t (min). k_1 (l/min) and k_2 (g/mg min) are the pseudo-first-order and pseudo-second-order rate constants. The values of parameters are calculated based on linear plots (Fig. 7 A & B) and are listed in Table 1. Hence, the high value of R^2 of linear plots (B) and value of Q_e (theoretical) were close to Q_e (experimental) In addition, the pseudo-second-order model was more favorable to describe the rate of lead ions uptake onto MGO@LaS nanocomposite.

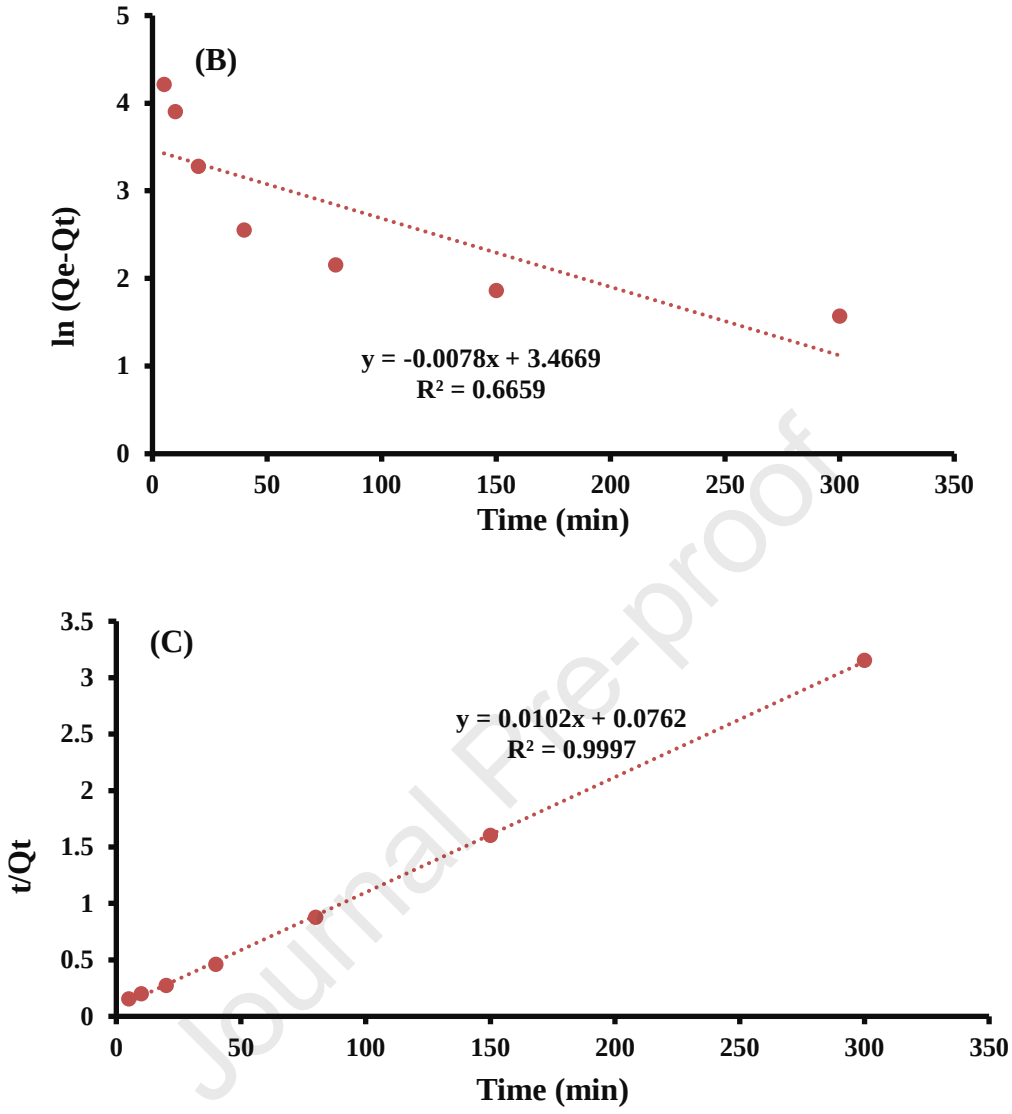

Fig. 7 (A) pseudo-first-order and (B) and pseudo-second-order kinetic models

Table.1 Kinetic parameters of the different models

Adsorbed	Q_e Experimental (mg/g)	Models					
		Pseudo first order			Pseudo second order		
		R^2	Q_e (mg/g)	k_1	R^2	Q_e (mg/g)	k_2
Pb(II)	90	0.665	31.08	0.007	0.999	98.03	0.0001

3.4 Adsorption equilibrium

3.4.1 Initial concentration of lead ions

Adsorption equilibrium of lead ions from wastewater was carried out for various initial concentrations of lead ions (5-200 mg/L) under constant shaking time, 20 mg adsorbent at pH 5. Fig. 8(A) shows an increasing the adsorption capacity with the increase of lead ions concentration. The proposed isotherm was compared with IUPAC pattern, which is the current isotherm is matched with IUPAC adsorption patterns that describe the monolayer Type I isotherm model. In addition, it can be noticed that the high concentrations of lead ions hindered further increase of the adsorption capacity due to the saturation of the active sites (Mohammadi Nodeh et al., 2020).

3.4.2 Adsorption isotherm

Adsorption capacity and adsorption pattern are studied through Langmuir and Freundlich isotherm models. The linear form of Langmuir and Freundlich models was described with equations (4) and (5) (Rashidi Nodeh et al., 2017).

$$C_e/Q_e = C_e/Q_m + 1/k_L Q_m \quad (4)$$

$$\ln Q_e = \ln K_F + (1/n) \ln C_e \quad (5)$$

Where Q_e (mg/g) is the equilibrium adsorption capacity (mg/g), Q_e is the maximum adsorption capacity, C_e (mg/L) is the concentration of lead ions before treatment, k_L is Langmuir constant (L/mg), K_F is Freundlich constant [(mg/g) $(L/mg)^{1/n}$] and $1/n$ is adsorption energy constant.

The value of the isotherm parameters was calculated from slopes and intercepts of the linear forms and plots (Fig. 8 B & C). Table 2 shows the Langmuir model was more favorable to describe the ions adsorption pattern over the MGO@LaS due to high values of R^2 as compared Freundlich model. Langmuir model was provided a satisfactory maximum adsorption capacity of 123 mg/g for lead ions at pH 5. Hence, the Langmuir model stated that the adsorption process was a monolayer on the surface of the adsorbent (Cechinel and de Souza, 2014; Ismail et al., 2016).

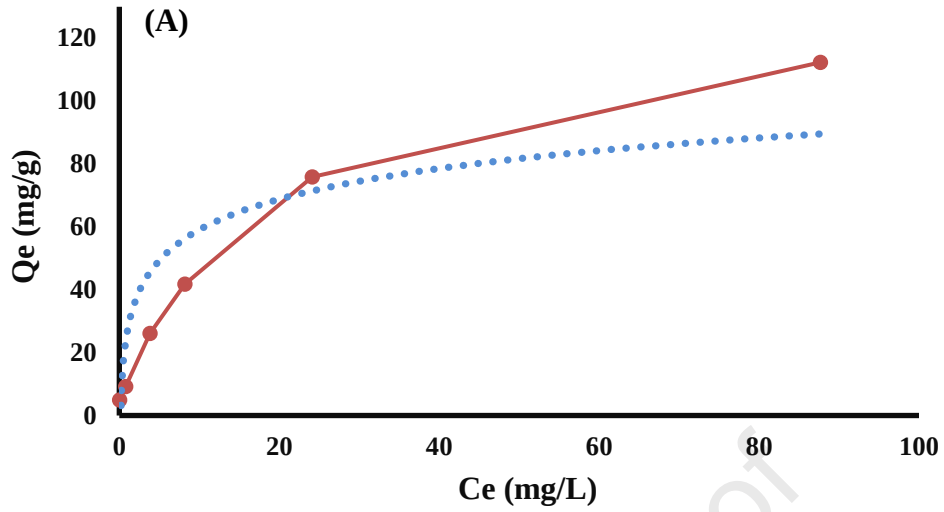

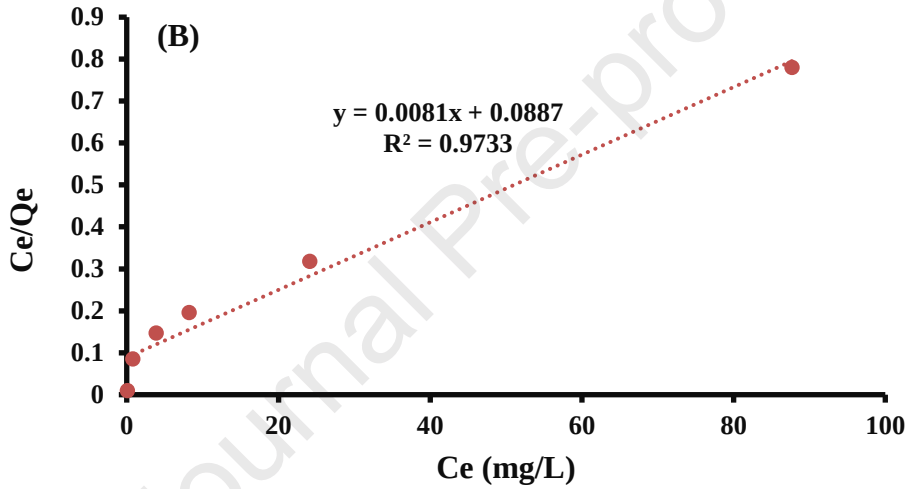

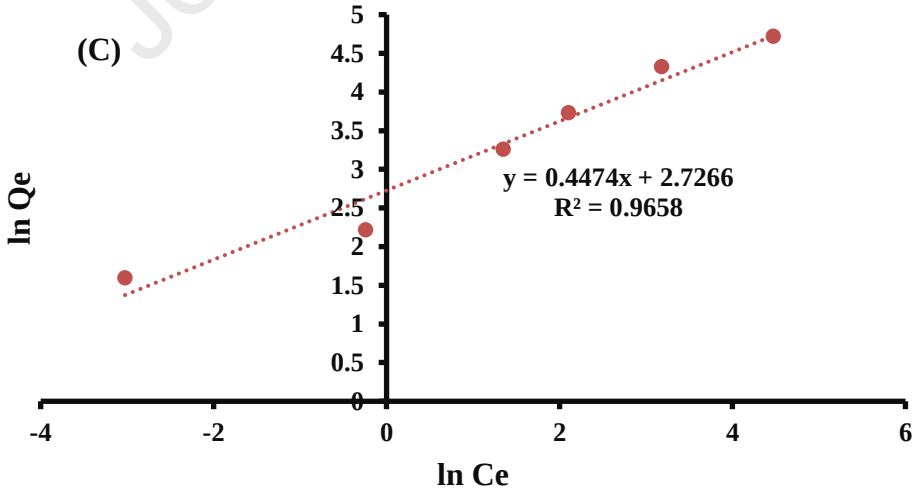

Fig. 8 (A) Adsorption equilibrium, (B) Langmuir and (C) Freundlich adsorption isotherms.

Table 2 Adsorption isotherms models and their parameter values.

Adsorbed	Models					
	Langmuir			Freundlich		
	Q_m (mg/g)	k_L	R^2	K_F[(mg/g) (L/mg)$^{1/n}$]	1/n	R^2
Pb(II)	123.46	0.91	0.973	12.74	2.23	0.965

3.5. Thermodynamic studies

The effect of temperature on lead ions adsorption onto MGO@LaS was investigated with the thermodynamic model as equations 5 and 6. The thermodynamic model describes the Gibbs free energy change (ΔG°), enthalpy change (ΔH°) and entropy change (ΔS°):

$$\Delta G° = -RT \ln K \quad (5)$$

$$\ln K = \frac{\Delta S°}{R} - \frac{\Delta H°}{RT} \quad (6)$$

where K = C_0/C_e (L/mol)R is the gas constant (8.314 J/mol K) and T is the temperature in Kelvin. In the linear form of the equation (*ln K versus 1/T*) the values of the ΔG°, ΔH° and ΔS° values are obtained from the slope and intercept of the linear plot and Listed in Table 3. It represents that the increase of adsorption capacity by temperature and positive value of ΔH° were performed the endothermic nature for lead adsorption process. A positive value of ΔS° suggests the randomness adoption pattern between the solid surface and solution. The negative ΔG° provided spontaneous adsorption of lead ions onto MGO@LaS nanocomposite. In addition, the value of ΔG° > -18 kJ mol^{-1} was performed chemisorption mechanism for lead ions onto MGO@LaS at 45 °C and chemisorption at 25 °C (ΔG° ~ -5.99 kJ mol^{-1}).

Table 3 Thermodynamic parameters for adsorption of Pb(II) ions onto MGO@LaS nanocomposite.

Target analyte	Temperature (K)	Q_e (mg/g)	ΔG° kJ mol^{-1}	ΔH° kJ mol^{-1}	ΔS° J mol^{-1} K^{-1}
Pb(II)	293	93.11	-2.92	181.23	0.61
	298	121.46	-5.99		
	318	133.21	-18.61		

3.6 Co-existing ions

The removal efficiency of lead ions using MGO@LaS was studied in the presence of various anions and cations (Section 2.4). After performing the co-existing ions, removal efficiency of 84 % was obtained for lead ions in the presence of various ions. In this case, the percentage of removal efficiency was unchanged significantly which means the ion was not competitive. It should be noted that some of the ions had negative effects which can decrease the removal efficiency due to the competitive adsorption and occupation of active sites by the onion or cations.

3.9 Comparison with other works

The results of this study were compared with previously published studies for the removal of lead. As can be seen in Table 4, the adsorbent of the current study displayed several advantages such as higher removal efficiency and mild adsorption condition as compared to some other adsorbents.

Table 4 Comparison study of lead ion sorption with different adsorbents

Adsorbent	Metal ion	pH	Q_e (mg/g)	Reference
MGO/LaS	lead	5	123.46	Current study
Magnetic biochar	lead	5	99.82	(Du et al., 2020b)
Zero valent Iron – Humic acid	lead	6	649	(Du et al., 2020a)
Magnetic GO	lead	4.5	86.2	(Rashidi Nodeh and Wan Ibrahim, 2016)
Amine-MOF	lead	4	536	(Mahmoud et al., 2020)
Bentonite biochar	Lead	4.2	500	(Ramola et al., 2020)
MGO/Chitosan	lead	5	76.94	(Fan et al., 2013)

4. Conclusion

A novel MGO@LaS nanocomposite was synthesized as an efficient adsorbent to enhance the removal of lead ions from wastewater. The results showed that the lead ions uptake onto MGO@LaS was well fitted by Langmuir isotherm ($R^2 > 0.99$) with a high adsorption capacity of 123.46 mg/g. In addition, the adsorption rate followed pseudo-second-order due to a higher R^2 (0.998) value as compared to pseudo-first-order. Lastly, Langmuir isotherm and thermodynamic modes (Gibes free energy) suggested a monolayer pattern for lead ions adsorption over

MGO@LaS with a chemical sorption mechanism at 45 ºC. The magnetic MGO@LaS nanocomposite provided an appropriate removal efficiency (85%) for lead ions in the presence of different anions and cations. Thus, the newly developed MGO@LaS nanocomposite can be used as an alternative solid sorbent material in water treatment.

Aknowledgment

The authors extend their appreciation to the Researchers Supporting Project number (RSP-2021/201), King Saud University, Riyadh, Saudi Arabia.

References

Ahmadi, K., Ghaedi, M., Ansari, A., 2015. Comparison of nickel doped Zinc Sulfide and/or palladium nanoparticle loaded on activated carbon as efficient adsorbents for kinetic and equilibrium study of removal of Congo Red dye. Spectrochim. Acta Part A Mol. Biomol. Spectrosc. 136, 1441–1449.

Anyakora, C., 2010. Heavy Metal Contamination of Ground Water : The Surulere Case Study. Res. J. Environ. Earth Sci. 2, 39–43.

Arbabi, M., Hemati, S., Amiri, M., 2015. Removal of lead ions from industrial wastewater: A review of Removal methods. Shahrekord Univ. Med. Sci. 2, 105–109.

Brandão, R.F., Quirino, R.L., Mello, V.M., Tavares, A.P., Peres, A.C., Guinhos, F., Rubim, J.C., Suarez, P.A.Z., 2009. Synthesis, characterization and use of Nb2O5 based catalysts in producing biofuels by transesterification, esterification and pyrolysis. J. Braz. Chem. Soc. 20, 954–966.

Cechinel, M.A.P., de Souza, A.A.U., 2014. Study of lead (II) adsorption onto activated carbon originating from cow bone. J. Clean. Prod. 65, 342–349.

Chai, W.S., Cheun, J.Y., Kumar, P.S., Mubashir, M., Majeed, Z., Banat, F., Ho, S.-H., Show, P.L., 2021. A review on conventional and novel materials towards heavy metal adsorption in wastewater treatment application. J. Clean. Prod. 126589.

Chakraborty, R., Asthana, A., Singh, A.K., Jain, B., Susan, A.B.H., 2020. Adsorption of heavy metal ions by various low-cost adsorbents: a review. Int. J. Environ. Anal. Chem. 1–38.

Du, Q., Li, G., Zhang, S., Song, J., Yang, F., 2020a. High-dispersion zero-valent iron particles stabilized by artificial humic acid for lead ion removal. J. Hazard. Mater. 383, 121170.

Du, Q., Zhang, S., Song, J., Zhao, Y., Yang, F., 2020b. Activation of porous magnetized biochar by artificial humic acid for effective removal of lead ions. J. Hazard. Mater. 389, 122115.

Duan, C., Ma, T., Wang, J., Zhou, Y., 2020. Removal of heavy metals from aqueous solution using carbon-based adsorbents: A review. J. Water Process Eng. 37, 101339.

Esmaeili Bidhendi, M., Abedynia, S., Mirzaei, S.S., Gabris, M.A., Rashidi Nodeh, H., Sereshti, H., 2020. Efficient removal of heavy metal ions from the water of oil- rich regions using layered metal- phosphate incorporated activated carbon nanocomposite. Water Environ. J. 34, 893–905.

Fan, L., Luo, C., Sun, M., Li, X., Qiu, H., 2013. Highly selective adsorption of lead ions by water-dispersible magnetic chitosan/graphene oxide composites. Colloids Surfaces B Biointerfaces 103, 523–529.

Fu, Z., Xi, S., 2020. The effects of heavy metals on human metabolism. Toxicol. Mech. Methods 30, 167–176.

Gabris, M.A., Jume, B.H., Rezaali, M., Shahabuddin, S., Rashidi Nodeh, H., Saidur, R., 2018. Novel magnetic graphene oxide functionalized cyanopropyl nanocomposite as an adsorbent for the removal of Pb (II) ions from aqueous media: equilibrium and kinetic studies. Environ. Sci. Pollut. Res. 25, 27122–27132. https://doi.org/10.1007/s11356-018-2749-9

Golkhah, S., ZAVVAR, M.H., Shirkhanloo, H., Khaligh, A., 2017. Removal of Pb (II) and Cu (II) ions from aqueous solutions by cadmium sulfide nanoparticles. Int. J. Nanosci. Nanotechnol. 13, 105–117.

Ismail, N.A., Bakhshaei, S., Kamboh, M.A., Abdul Manan, N.S., Mohamad, S., Yilmaz, M., 2016. Adsorption of phenols from contaminated water through titania-silica mixed imidazolium based ionic liquid: Equilibrium, kinetic and thermodynamic modeling studies. J. Macromol. Sci. Part A 53, 619–628.

Jun, B.-M., Kim, S., Kim, Y., Her, N., Heo, J., Han, J., Jang, M., Park, C.M., Yoon, Y., 2019. Comprehensive evaluation on removal of lead by graphene oxide and metal organic framework. Chemosphere 231, 82–92.

Kakavandi, B., Kalantary, R.R., Jafari, A.J., Nasseri, S., Ameri, A., Esrafili, A., Azari, A., 2015. Pb (II) adsorption onto a magnetic composite of activated carbon and superparamagnetic Fe3O4 nanoparticles: Experimental and modeling study. CLEAN–Soil, Air, Water 43, 1157–1166.

Kamboh, M.A., Arain, S.S., Jatoi, A.H., Sherino, B., Algarni, T.S., Al-onazi, W.A., Al-Mohaimeed, A.M., Rezania, S., 2021. Green sporopollenin supported cyanocalixarene based magnetic adsorbent for pesticides removal from water: Kinetic and equilibrium studies. Environ. Res. 25, 111588.

Lai, K.C., Lee, L.Y., Hiew, B.Y.Z., Thangalazhy-Gopakumar, S., Gan, S., 2020. Facile synthesis of xanthan biopolymer integrated 3D hierarchical graphene oxide/titanium dioxide composite for adsorptive lead removal in wastewater. Bioresour. Technol. 309, 123296.

Leong, Y.K., Chang, J.-S., 2020. Bioremediation of heavy metals using microalgae: Recent advances and mechanisms. Bioresour. Technol. 303, 122886.

Li, Y., Cao, L., Li, L., Yang, C., 2015. In situ growing directional spindle TiO2 nanocrystals on cellulose fibers for enhanced Pb(2+) adsorption from water. J. Hazard. Mater. 289, 140–8. https://doi.org/10.1016/j.jhazmat.2015.02.051

Li, Yuxin, Zhang, D., Li, W., Lan, Y., Li, Ying, 2020. Efficient removal of As (III) from aqueous solution by S-doped copper-lanthanum bimetallic oxides: Simultaneous oxidation and adsorption. Chem. Eng. J. 384, 123274.

Madhavan, J., Theerthagiri, J., Balaji, D., Sunitha, S., Choi, M.Y., Ashokkumar, M., 2019. Hybrid advanced oxidation processes involving ultrasound: an overview. Molecules 24, 3341.

Mahmoud, M.E., Amira, M.F., Seleim, S.M., Mohamed, A.K., 2020. Amino-decorated magnetic metal-organic framework as a potential novel platform for selective removal of chromium (Vl), cadmium (II) and lead (II). J. Hazard. Mater. 381, 120979.

Mohammadi Nodeh, M.K., Bidhendi, G.N., Gabris, M.A., Akbari-adergani, B., Rashidi Nodeh, H., Masoudi, A., Shahabuddin, S., 2020. Strontium oxide decorated iron oxide activated carbon nanocomposite: a new adsorbent for removal of nitrate from well water. J. Braz. Chem. Soc. 31, 116–125.

Mousavi, S.V., Bozorgian, A., Mokhtari, N., Gabris, M.A., Nodeh, H.R., Ibrahim, W.A.W., 2019. A novel cyanopropylsilane-functionalized titanium oxide magnetic nanoparticle for the adsorption of nickel and lead ions from industrial wastewater: Equilibrium, kinetic and thermodynamic studies. Microchem. J. 145, 914–920.

Muthusaravanan, S., Balasubramani, K., Suresh, R., Ganesh, R.S., Sivarajasekar, N., Arul, H., Rambabu, K., Bharath, G., Sathishkumar, V.E., Murthy, A.P., 2021. Adsorptive removal of

noxious atrazine using graphene oxide nanosheets: Insights to process optimization, equilibrium, kinetics, and density functional theory calculations. Environ. Res. 111428.

Naik, S.S., Lee, S.J., Theerthagiri, J., Yu, Y., Choi, M.Y., 2021. Rapid and highly selective electrochemical sensor based on ZnS/Au-decorated f-multi-walled carbon nanotube nanocomposites produced via pulsed laser technique for detection of toxic nitro compounds. J. Hazard. Mater. 126269.

Paithankar, J.G., Saini, S., Dwivedi, S., Sharma, A., Chowdhuri, D.K., 2021. Heavy metal associated health hazards: An interplay of oxidative stress and signal transduction. Chemosphere 262, 128350.

Pandian, S.R.K., Deepak, V., Kalishwaralal, K., Gurunathan, S., 2011. Biologically synthesized fluorescent CdS NPs encapsulated by PHB. Enzyme Microb. Technol. 48, 319–325.

Patil, S.J., Lokhande, C.D., 2015. Fabrication and performance evaluation of rare earth lanthanum sulfide film for supercapacitor application: effect of air annealing. Mater. Des. 87, 939–948.

Prabhu, S.M., Park, C.M., Shahzad, A., Lee, D.S., 2019. Designed synthesis of sulfide-rich bimetallic-assembled graphene oxide sheets as flexible materials and self-tuning adsorption cum oxidation mechanisms of arsenic from water. J. Mater. Chem. A 7, 12253–12265.

Rajivgandhi, G., Vimala, R.T. V, Nandhakumar, R., Murugan, S., Alharbi, N.S., Kadaikunnan, S., Khaled, J.M., Alanzi, K.F., Li, W.-J., 2021. Adsorption of nickel ions from electroplating effluent by graphene oxide and reduced graphene oxide. Environ. Res. 199, 111322.

Ramola, S., Belwal, T., Li, C.J., Wang, Y.Y., Lu, H.H., Yang, S.M., Zhou, C.H., 2020. Improved lead removal from aqueous solution using novel porous bentonite-and calcite-biochar composite. Sci. Total Environ. 709, 136171.

Ramu, A.G., Telmenbayar, L., Theerthagiri, J., Yang, D., Song, M., Choi, D., 2020. Synthesis of a hierarchically structured Fe 3 O 4–PEI nanocomposite for the highly sensitive electrochemical determination of bisphenol A in real samples. New J. Chem. 44, 18633–18645.

Rashidi Nodeh, H., Sereshti, H., Beirakabadi, E., Razmkhah, K., 2020a. Synthesis and application of lanthanum sulfide nanoparticles for removal of tetracycline from aqueous media. Int. J. Environ. Sci. Technol. 17, 819–828.

Rashidi Nodeh, H., Sereshti, H., Zamiri Afsharian, E., Nouri, N., 2017. Enhanced removal of phosphate and nitrate ions from aqueous media using nanosized lanthanum hydrous doped on magnetic graphene nanocomposite. J. Environ. Manage. 197. https://doi.org/10.1016/j.jenvman.2017.04.004

Rashidi Nodeh, H., Shakiba, M., Gabris, M.A., Bidhenda, M.E., Shahabuddin, S., Khanam, R., 2020b. Spherical iron oxide methyltrimethoxysilane nanocomposite for the efficient removal of lead (II) ions from wastewater: kinetic and equilibrium studies. Desalin. WATER Treat. 192, 297–305.

Rashidi Nodeh, H., Wan Ibrahim, W.A., 2016. Magnetic graphene oxide as adsorbent for the removal of lead (II) from water samples. J. Teknol. 78, 3–2.

Senthil, R.A., Priya, A., Theerthagiri, J., Selvi, A., Nithyadharseni, P., Madhavan, J., 2018. Facile synthesis of α-Fe 2 O 3/WO 3 composite with an enhanced photocatalytic and photo-electrochemical performance. Ionics (Kiel). 24, 3673–3684.

Shirani, M., Kamboh, M.A., Akbari-Adergani, B., Akbari, A., Arain, S.S., Rashidi Nodeh, H., 2021. Sonodecoration of magnetic phosphonated-functionalized sporopollenin as a novel green nanocomposite for stir bar sorptive dispersive microextraction of melamine in milk and milk-based food products. Food Chem. 341, 128460.

Tan, Z., Wu, W., Feng, C., Wu, H., Zhang, Z., 2020. Simultaneous determination of heavy metals by an electrochemical method based on a nanocomposite consisting of fluorinated graphene and gold nanocage. Microchim. Acta 187, 1–9.

Theerthagiri, J., Senthil, R.A., Senthilkumar, B., Polu, A.R., Madhavan, J., Ashokkumar, M., 2017. Recent advances in MoS2 nanostructured materials for energy and environmental applications–a review. J. Solid State Chem. 252, 43–71.

Wan Ibrahim, W.A., Rashidi Nodeh, H., Sanagi, M.M., 2016. Graphene-Based Materials as Solid Phase Extraction Sorbent for Trace Metal Ions, Organic Compounds, and Biological Sample Preparation. Crit. Rev. Anal. Chem. 46, 267–283. https://doi.org/10.1080/10408347.2015.1034354

Wu, G., Ma, J., Li, S., Wang, S., Jiang, B., Luo, S., Li, J., Wang, X., Guan, Y., Chen, L., 2020. Cationic metal-organic frameworks as an efficient adsorbent for the removal of 2, 4-dichlorophenoxyacetic acid from aqueous solutions. Environ. Res. 186, 109542.

Wu, K., Jing, C., Zhang, J., Liu, T., Yang, S., Wang, W., 2019. Magnetic Fe3O4@ CuO

nanocomposite assembled on graphene oxide sheets for the enhanced removal of arsenic (III/V) from water. Appl. Surf. Sci. 466, 746–756.

Yu, Y., Naik, S.S., Oh, Y., Theerthagiri, J., Lee, S.J., Choi, M.Y., 2021. Lignin-mediated green synthesis of functionalized gold nanoparticles via pulsed laser technique for selective colorimetric detection of lead ions in aqueous media. J. Hazard. Mater. 420, 126585.

Zhang, Q., Hou, Q., Huang, G., Fan, Q., 2020. Removal of heavy metals in aquatic environment by graphene oxide composites: a review. Environ. Sci. Pollut. Res. 27, 190–209.

Zhao, Y., Tian, S., Gong, Y., Zhao, D., 2019. Efficient Removal of Lead from Water Using Stabilized Iron Sulfide Nanoparticles: Effectiveness and Effects of Stabilizer. Water, Air, Soil Pollut. 230, 1–14.

Highlights

- Lanthanum sulfide nanoparticles were synthesized and decorated on magnetic graphene oxide.
- The MGO@LaS nanocomposite applied for removal of lead ions (Pb2+) from wastewater.
- The isotherm model provided monolayer adsorption for lead ions with an adsorption capacity of 123.46 mg/g.

Declaration of interests

☒ The authors declare that they have no known competing financial interests or personal relationships that could have appeared to influence the work reported in this paper.

☐The authors declare the following financial interests/personal relationships which may be considered as potential competing interests: